Metal chalcogenide nanorings for temperature-strain dual-mode sensing

Xiaoshan Wang[a,b,c], Jinhao Zhang[a], Peiyuan Liu[c], Danlin Wei[b], Daobo Tian[b], Shipeng Liu[c], Qian Chen[c], Jiacheng Cao[c], Zhiwei Wang[a,c], Xiao Huang[a*]

[a] Institute of Advanced Materials (IAM), School of Flexible Electronics (SoFE), Nanjing Tech University (NanjingTech), 30 South Puzhu Road, Nanjing 211816, China

[b] Ningxia Key Laboratory of Photovoltaic Materials, School of Materials and New Energy, Ningxia University, Yinchuan 750021, China

[c] Frontiers Science Center for Flexible Electronics, Xi'an Institute of Flexible Electronics (IFE) and Xi'an Institute of Biomedical Materials & Engineering, Northwestern Polytechnical University, 127 West Youyi Road, Xi'an 710072, China

*Corresponding author. iamxhuang@njtech.edu.cn, iamwhuang@nwpu.edu.cn

Characterization methods.

Scanning electron microscope (SEM, JEOL JSM-7800F, Japan), transmission electron microscope (TEM, JEOL 2100Plus, Japan), high resolution transmission electron microscope (HRTEM, JEOL 2100F, Japan) coupled with energy dispersive X-ray (EDX) spectroscope were used to investigate the materials morphological, compositional, and structural features. X-ray diffraction (XRD, Rigaku SmartLab, Japan) and X-ray photoelectron spectroscopy (XPS, PHI 5000 VersaProbe, Japan) were performed to reveal the materials crystal phase and structure. Raman spectra (Horiba HR800, France) were obtained with a 532 nm laser. The metallic properties of the $Sn_{0.2}Mo_{0.8}S_2$ nanorings were studied with a semiconductor characterization system (Keithley 4200).

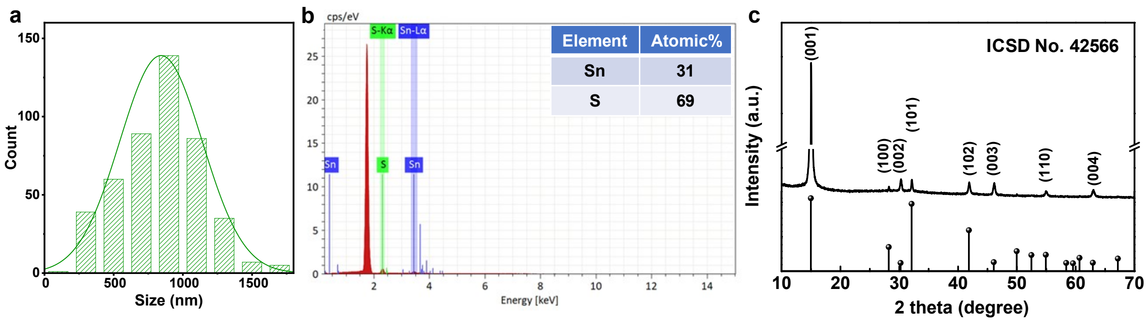

Fig. S1 EDX analysis (a) and XRD pattern (b) of SnS_2 nanoplates.

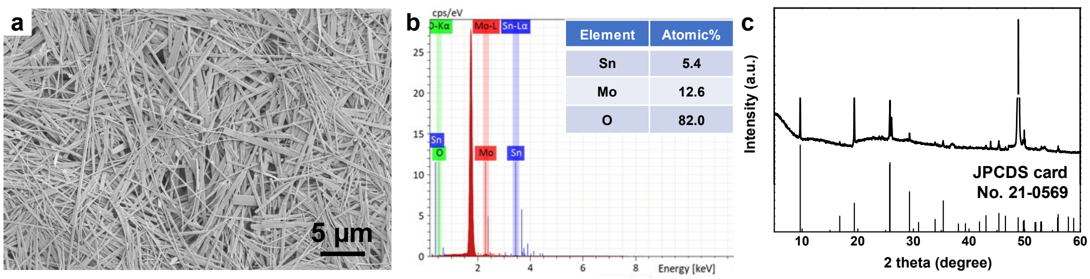

Fig. S2 SEM image (a), EDX analysis (b), and XRD pattern (c) of $Sn_{0.3}Mo_{0.7}O_3$ nanorods.

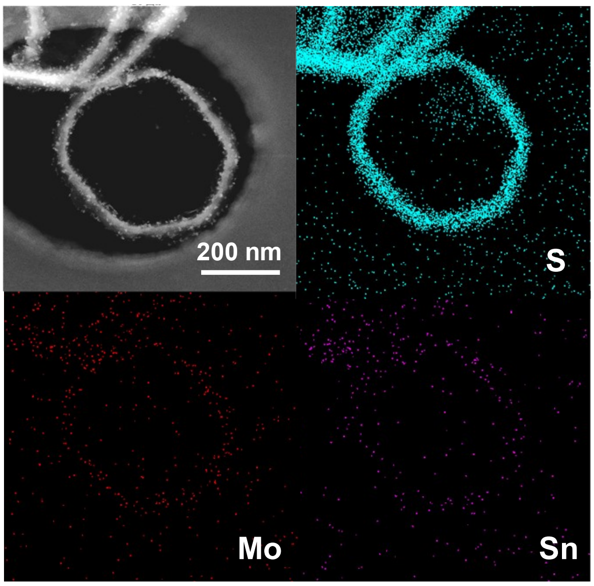

Fig. S3 STEM image and EDX mapping of $Sn_{1-x}Mo_xS_2$ nanorings.

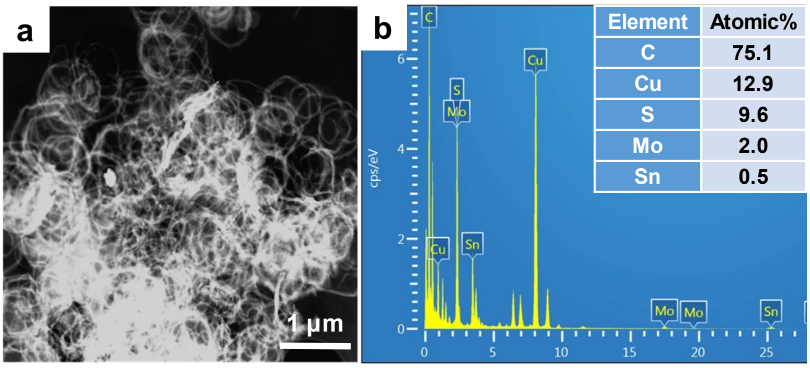

Fig. S4 STEM image (a) and EDX spectrum (b) of $Sn_{0.2}Mo_{0.8}S_2$ nanorings. A mean value of ~0.8 was determined for x.

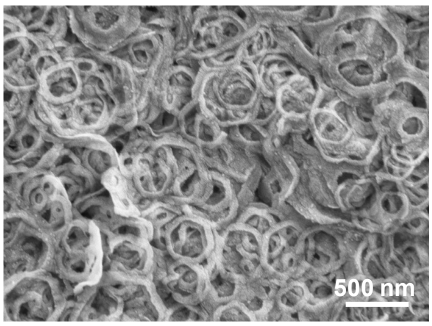

Fig. S5 The SEM images of $Sn_{0.2}Mo_{0.8}S_2$ nanorings were synthesized 12 mg $Sn_{0.3}Mo_{0.7}O_3$ as precursors.

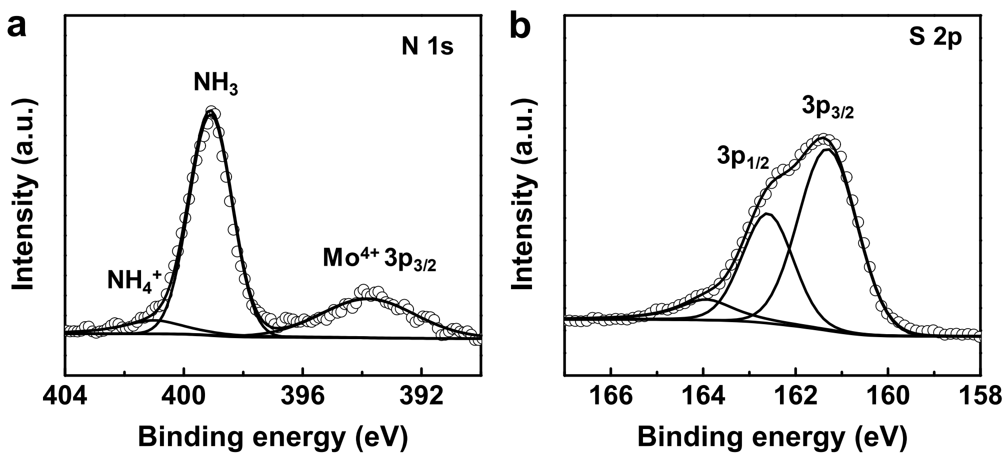

Fig. S6 XPS N 1s (a) and S 2p (b) spectra of $Sn_{0.2}Mo_{0.8}S_2$ nanorings.

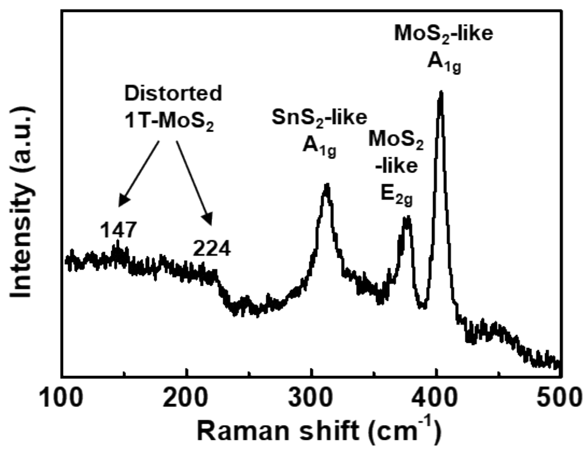

Fig. S7 Raman spectrum of $Sn_{0.2}Mo_{0.8}S_2$ nanorings.

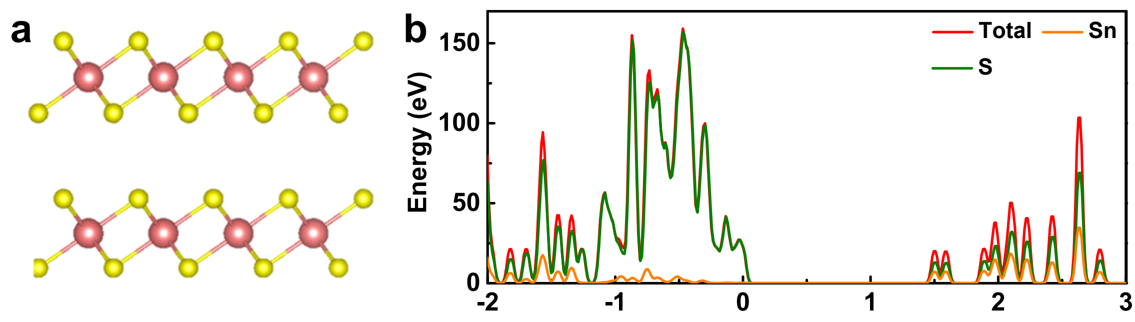

Fig. S8 Optimized crystal structure (a) and DOS (b) of a SnS_2, showing the semiconducting property. The Fermi level is assigned at 0 eV.

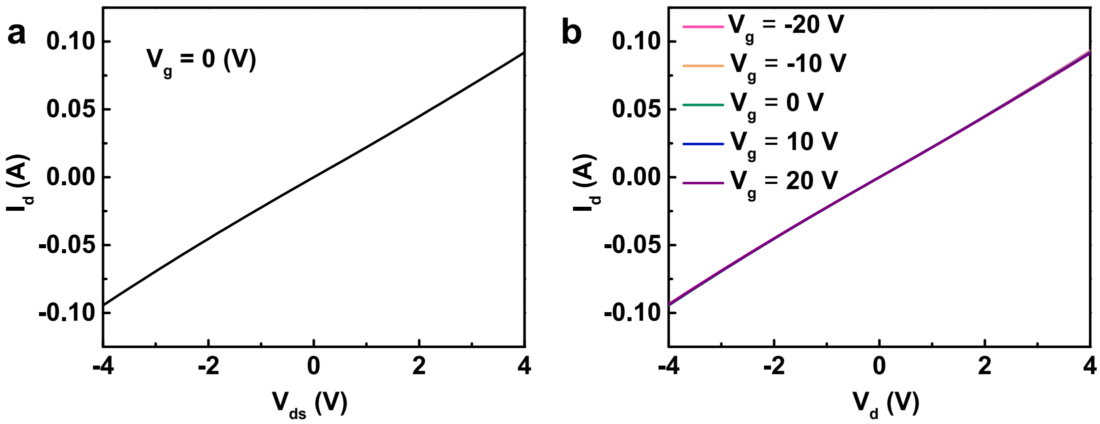

Fig. S9 Drain current (I_d) characteristics of back-gated TFTs based $Sn_{0.2}Mo_{0.8}S_2$ nanorings for drain-source voltages (V_{ds}) varied from -4 to 4 V at 0 V gate voltage (V_g). The I_d-V_{ds} curves of $Sn_{0.2}Mo_{0.8}S_2$ nanorings at varied V_g from -20 to 20 V.

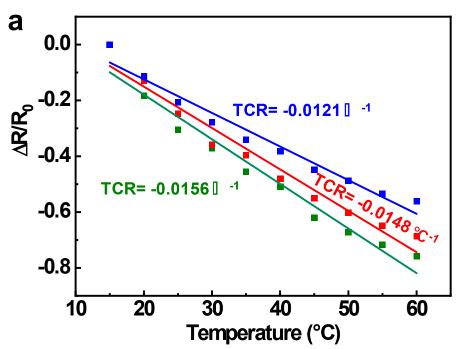

b

Radius of curvature (mm)	TCR (℃$^{-1}$)
52.8	-0.0121
41.7	-0.0148
35.1	-0.0156

Fig. S10 (a) Calculation of temperature coefficient of resistance. (b) TCR of temperature sensors with different radius of curvature.

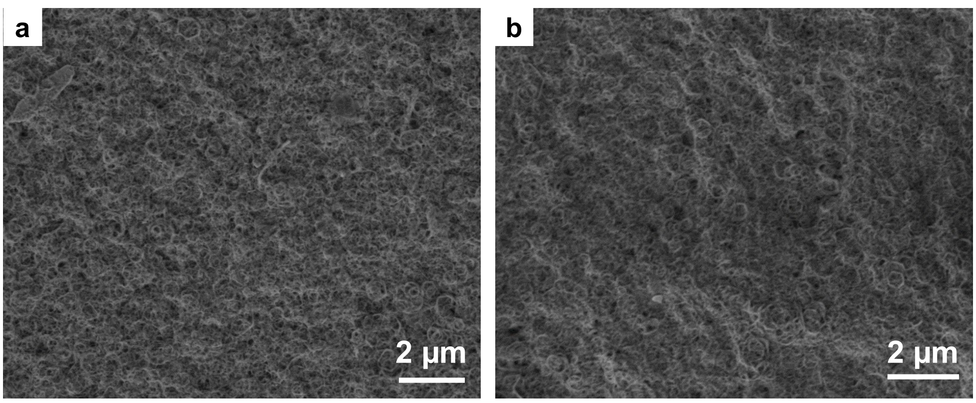

Fig. S11 The SEM images of $Sn_{0.2}Mo_{0.8}S_2$ nanorings based strain sensor before (a) and after (b) 300 cyclic bending tests.

Table 1 Comparison of various inorganic materials-based thermoresistive temperature sensors.

Material type	Material	Fabrication method	Temperature range (℃)	Sensitivity	Stretchability	Ref.
Carbon	$Sn_{0.2}Mo_{0.8}S_2$	inkjet printing	25-85	-0.013 $℃^{-1}$	flexible	This work
	rGO fiber	wet spinning	30-80	-0.00636 $℃^{-1}$	flexible	1
	rGO-PU/PDMS	wet spinning	25-50	-0.01185 $℃^{-1}$	50%	2
	rGO film	spray coating	0-100	-	3%	3
	graphene-(PEDOT:PSS)/PU	inkjet printing	35-45	-0.0006 $℃^{-1}$	-	4
	rGO/parlylene	spray coating	22-70	-0.0083 $℃^{-1}$	flexible	5
	rGO/PET	spray coating	30-100	-0.006345 $℃^{-1}$	flexible	6
	PEI-rGO/polyimide	Spray coating	25-45	-0.013 $℃^{-1}$	bending angle:40°	7
	graphene/ polyorganosiloxane aerogels	freeze drying	20-100	-	80%	8
	graphene nanoribbons	writing or spraying	30-80	-0.0127 $℃^{-1}$	curvature radius: 1 cm	9
	graphene/porous elastic polyurethane	dip coating	20-100	-0.00815 $℃^{-1}$	50%	10
	rGO-Pu	spin coating	-	0.009 $℃^{-1}$	70%	11
	CNT	printing	21-80	~0.0025 $℃^{-1}$	flexible	12
	graphene	CVD	-	0.0042 $℃^{-1}$	40%	13
	$Ti_3C_2T_x$/cellulose	vacuum filtration	27-140	~0.00222 $℃^{-1}$	flexible	14
	LIG/MXene-$Ti_3C_2T_x$@EDOT	laser-induced	26-45	0.0052 K^{-1}	flexible	15
metal nanowire	Ag NWs	electrospinning	30-45	0.0003 $℃^{-1}$	flexible	16
	Ag NWs-PI	filtration	-20-20	0.0033 $℃^{-1}$	flexible	17
semiconductor	MoS_2	CVD	27-120	0.01-0.02 K^{-1}	flexible	18
	MoS_2	-	-	0.0057 K^{-1}	-	19
	$MoTe_2$	-	-	0.0064 K^{-1}	-	19
	MoS_2-graphene	coating	-	-	flexible	20
	MoS_2	printing	-	0.0102 $℃^{-1}$	80%	21
	MoS_2	inkjet printing	30-70	-0.0095 $℃^{-1}$	flexible	22

Referance

1 T. Q. Trung, H. S. Le, T. M. L. Dang, S. Ju, S. Y. Park and N. E. Lee, *Adv. Healthc. Mater.*, 2018, **7**, e1800074.

2 T. Q. Trung, T. M. L. Dang, S. Ramasundaram, P. T. Toi, S. Y. Park and N. E. Lee, *ACS Appl. Mater. Interfaces*, 2019, **11**, 2317-2327.

3 D. H. Ho, Q. Sun, S. Y. Kim, J. T. Han, D. H. Kim and J. H. Cho, *Adv. Mater.*, 2016, **28**, 2601-2608.

4 T. Vuorinen, J. Niittynen, T. Kankkunen, T. M. Kraft and M. Mantysalo, *Sci. Rep.*, 2016, **6**, 35289.

5 G. Y. Bae, J. T. Han, G. Lee, S. Lee, S. W. Kim, S. Park, J. Kwon, S. Jung and K. Cho, *Adv. Mater.*, 2018, **30**, e1803388.

6 G. Liu, Q. Tan, H. Kou, L. Zhang, J. Wang, W. Lv, H. Dong and J. Xiong, *Sensors*, 2018, **18**

7 Q. Liu, H. Tai, Z. Yuan, Y. Zhou, Y. Su and Y. Jiang, *Adv. Mater.Technol.*, 2019, **4**

8 G. Zu, K. Kanamori, K. Nakanishi and J. Huang, *Chem. Mater.*, 2019, **31**, 6276-6285.

9 X. Gong, L. Zhang, Y. Huang, S. Wang, G. Pan and L. Li, *RSC Adv.*, 2020, **10**, 22222-22229.

10 X. Hu, M. Tian, T. Xu, X. Sun, B. Sun, C. Sun, X. Liu, X. Zhang and L. Qu, *ACS Nano*, 2020, **14**, 559-567.

11 T. Q. Trung, S. Ramasundaram, B. U. Hwang and N. E. Lee, *Adv. Mater.*, 2016, **28**, 502-509.

12 S. Harada, K. Kanao, Y. Yamamoto, T. Arie, S. Akita and K. Takei, *ACS Nano*, 2014, **8**, 12851-12857.

13 S. Kabiri Ameri, R. Ho, H. Jang, L. Tao, Y. Wang, L. Wang, D. M. Schnyer, D. Akinwande and N. Lu, *ACS Nano*, 2017, **11**, 7634-7641.

14 V. Adepu, V. Mattela and P. Sahatiya, *J Mater. Chem. B*, 2021, **9**, 4523-4534.

15 S. Zhang, A. Chhetry, M. A. Zahed, S. Sharma, C. Park, S. Yoon and J. Y. Park, *npj Flex. Electron.*, 2022, **6**

16 B. W. An, S. Heo, S. Ji, F. Bien and J. U. Park, *Nat. Commun.*, 2018, **9**, 2458.

17 D. Y. Youn, U. Jung, M. Naqi, S. J. Choi, M. G. Lee, S. Lee, H. J. Park, I. D. Kim and S. Kim, *ACS Appl. Mater. Interfaces*, 2018, **10**, 44678-44685.

18 A. Daus, M. Jaikissoon, A. I. Khan, A. Kumar, R. W. Grady, K. C. Saraswat and E. Pop, *Nano Lett.*, 2022, **22**, 6135-6140.

19 A. I. Khan, P. Khakbaz, K. A. Brenner, K. K. H. Smithe, M. J. Mleczko, D. Esseni and E. Pop, *Appl. Phys. Lett.*, 2020, **116**

20 Y. Xie, T.-M. Chou, W. Yang, M. He, Y. Zhao, N. Li and Z.-H. Lin, *Semicond. Sci. Technol.*, 2017, **32**

21 Y. Lu, J. Wang, J. He, L. Zou, D. Zhao and S. Song, *ACS Appl. Mater. Interfaces*, 2022, **14**, 29250-29260.

22 W. Li, M. Xu, J. Gao, X. Zhang, H. Huang, R. Zhao, X. Zhu, Y. Yang, L. Luo, M. Chen, H. Ji, L. Zheng, X. Wang and W. Huang, *Adv. Mater.*, 2023, **35**, e2207447.